

state [7]. The measured wavelength was 0.9463 μm . When the laser facets were coated to $R \approx 0.99$, the threshold dropped by $\times 10$. It operated in the first quantised state with a lasing wavelength of 1.0102 μm .

Fourthly, low threshold lasers can be tailored for different applications. The laser with 165 μA threshold current had very low external quantum efficiency of 0.005 mW/mA. This is due to the very high mirror reflectivities (estimated as higher than 0.99). For some applications more optical power and higher external quantum efficiency may be preferred. In these cases, the reflectivity of one mirror should be relaxed. Fig. 3 shows the L-I curve of another low threshold laser. The cavity length of the laser was 120 μm and the mirror reflectivities were $R_r = 0.92$, $R_f = 0.99$. The room temperature CW threshold current of the laser was 0.28 mA, but the external quantum efficiency increased to 0.3 mW/mA. An example of the high power operation of low threshold lasers is as follows: the cavity length of the laser was 200 μm , the rear facet mirror was coated to $R_r = 0.99$ ($R_f \approx 0.3$). The CW threshold of the laser was 0.65 mA and the front facet external quantum efficiency was 0.66 mW/mA. More than 30 mW linear optical power was delivered from the uncoated front facet.

In conclusion, a room temperature CW threshold current of 165 μA and cryogenic temperature (6 K) threshold current of 21 μA have been demonstrated in a BH SL SQW InGaAs/AlGaAs laser with 125 μm cavity length and ~ 0.99 mirror reflectivities.

Acknowledgments: This work was supported by the Office of Naval Research, ARPA, and the Air Force Office of Scientific Research.

© IEE 1995

12 December 1994

Electronics Letters Online No: 19950176

T.R. Chen, B. Zhao, L. Eng, J. Feng, Y.H. Zhuang and A. Yariv (California Institute of Technology, Pasadena, CA 91125, USA)

References

- 1 SIN, Y.K., HORIKAWA, H., MATSUI, Y., and KAMIJOH, T.: 'Ultra-low laser threshold and high-speed InGaAs/GaAs/InGaP buried heterostructure strained-quantum-well lasers for optical interconnects', *Electron. Lett.*, 1993, **29**, pp. 873-875
- 2 CHEN, T.R., ENG, L., ZHAO, B., ZHANG, Y.H., and YARIV, A.: 'Strained single-quantum-well InGaAs lasers with a threshold current of 0.25 mA', *Appl. Phys. Lett.*, 1993, **63**, pp. 2621-2623
- 3 ZHAO, H., MACDOUGAL, M.H., UPPAL, K., and DAPKUS, D.: 'Sub-milliampere threshold InGaAs/GaAs/AlGaAs laser array elements by single step growth on nonplanar substrates', 14th IEEE Int. Semiconductor Laser Conf., 1994, pp. 18
- 4 ZOU, W.X., BOWEN, T., LAW, K.K., YOUNG, D.B., and METZ, J.L.: '1.0 mA-threshold uncoated lasers by impurity-induced disordering', *IEEE Photonics Technol. Lett.*, 1993, **5**, pp. 591-594
- 5 ZHAO, B., CHEN, T.R., and YARIV, A.: 'Effect of state filling on the modulation response and threshold current of quantum-well lasers', *Appl. Phys. Lett.*, 1992, **60**, pp. 1930-1932
- 6 KUROBE, A., FURUYAMA, H., NARITSUKA, S., SUGIYAMA, N., KOKUBUN, Y., and NAKAMURA, M.: 'Effects of well number, cavity length, and facet reflectivity on the reduction of threshold current of GaAs/AlGaAs multiquantum well lasers', *IEEE J. Quantum Electron.*, 1988, **QE-24**, pp. 635-639
- 7 BEERMINK, K.J., ALWAN, J.J., and COLEMAN, J.J.: 'Wavelength switching in narrow oxide stripe InGaAs/GaAs/AlGaAs strained-layer quantum-well heterostructure lasers', *Appl. Phys. Lett.*, 1991, **58**, pp. 2067-2078

Self-starting soliton modelocked Ti-sapphire laser using a thin semiconductor saturable absorber

L.R. Brovelli, I.D. Jung, D. Kopf, M. Kamp, M. Moser, F.X. Kärtner and U. Keller

Indexing terms: Solid lasers, Laser mode locking

Using a 15 nm-thick antireflection-coated GaAs absorber layer on an AlGaAs/AlAs Bragg mirror as a nonlinear reflector, we achieved self-starting passive modelocking of a Ti-sapphire laser with 34 fs pulses without Kerr lens modelocking.

The discovery of Kerr lens modelocking (KLM) [1] has stimulated intensive research in the area of passively modelocked solid-state lasers over the past several years. Currently, the shortest pulses obtained directly from a laser (8.5 fs) have been achieved with a KLM Ti-sapphire laser [2]. KLM, however, is generally not self-starting because it scales with peak intensities. Most KLM experiments therefore rely on an active starting mechanism such as a shaking mirror or a regenerative active modelocker. Self-starting KLM pulses with durations longer than 50 fs have been obtained from specially designed cavities very close to the limit of the stability regime [3, 4], and therefore with very critical alignment tolerances. In contrast, it has been demonstrated that a slow saturable absorber could be used as a starting mechanism [5].

Semiconductor saturable absorbers seem very promising because they are compact, inexpensive, and cover a wide wavelength range from the visible to the infra-red. In general, however, they introduce too much loss, saturate too easily, and have too low a damage threshold. All these issues can be solved by use of the antiresonant Fabry-Perot saturable absorber (A-FPSA), which sandwiches the absorber between two Bragg mirrors, forming a Fabry-Perot cavity with an antiresonance at the wavelength of interest [6, 7]. This antiresonant design decreases the losses introduced in the cavity and increases the saturation intensity and the damage threshold. The saturable absorber parameters of an A-FPSA can be fully designed to give optimum modelocking performance [8]. The design parameters of the A-FPSA are absorber bandgap, thickness of absorber, carrier lifetime and the top reflector. Many different solid-state lasers have been successfully modelocked using an A-FPSA.

Given our understanding of the A-FPSA's parameters, we can scale the device to thinner saturable absorber layers, which in turn requires a decrease in the top reflector to couple more light into the device and maintain the same saturation behaviour. In this work, we take this scaling to the limit where we have a very thin saturable absorber and an antireflection coating on the top (instead of a high-reflector) to fully couple the laser light into the device. Our modelling has shown we could fabricate this device with bleached losses of $\sim 5\%$, which is acceptable for typical Ti:sapphire lasers. To prevent significant CW saturation the laser spot size on the absorber has to be increased compared to an A-FPSA design. We used a thin (15 nm) GaAs saturable absorber layer on an AlGaAs/AlAs Bragg mirror as a nonlinear reflector (Fig. 1) in an argon-ion pumped Ti:sapphire laser, achieving self-starting 34 fs pulses in a regime where KLM is insignificant or even counteracts pulse formation. The pulse generation is based on soliton modelocking [9].

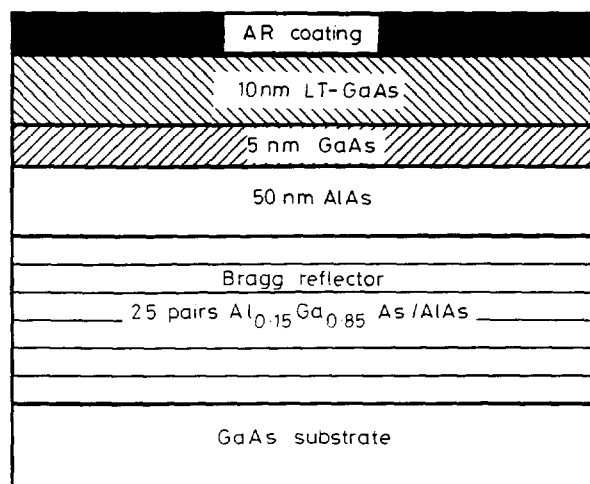


Fig. 1 Structure of a nonlinear semiconductor saturable absorber Bragg reflector

Not to scale

The device (Fig. 1) incorporates a Bragg mirror with 25 pairs of AlAs/Al_{0.15}Ga_{0.85}As grown by metal-organic chemical vapour phase deposition (MOCVD) on a GaAs substrate giving a maximum reflectivity of 99.5% (Fig. 2). A 50 nm-thick AlAs spacer was grown by molecular beam epitaxy (MBE) on top of the mirror, which shifts the absorber layer into a maximum of the standing

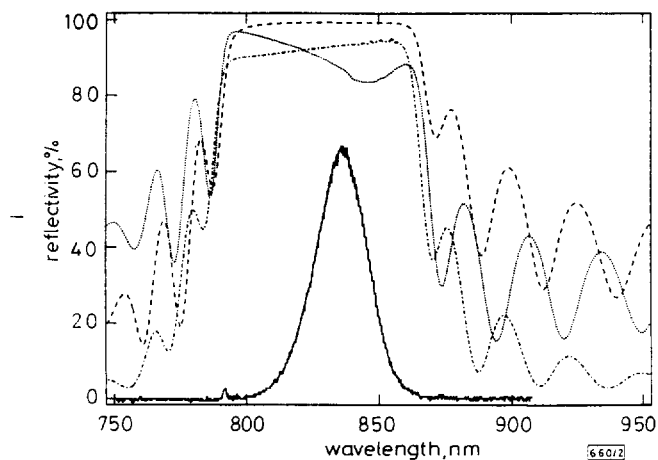


Fig. 2 Low-intensity reflectivity of uncoated absorber, AR-coated absorber and Bragg mirror, and spectrum of mode-locked pulses

..... uncoated sample
 - - - - AR-coated sample
 - · - · Bragg mirror
 ——— pulse spectrum

wave. The absorber consists of 5 nm GaAs grown at normal temperature (i.e. 600°C) and of 10 nm GaAs grown at 350°C. Growth at lower temperatures (LT-growth) leads to incorporation of excess arsenic introducing crystal defects and shortening the carrier lifetime, and therefore the absorber recovery time. For GaAs grown at 350°C, we measured a lifetime of 10–12 ps using a standard noncollinear pump-probe setup. Reducing the absorber recovery time increases the CW-saturation intensity and makes the laser more stable against self-Q-switching [5, 8]. On the other hand, the longer carrier lifetime of the normal-grown GaAs layer supports self-starting modelocking. Finally an AR coating was required in order to eliminate the Fabry-Perot resonance at ~840 nm, resulting in a reflectivity that is almost flat within the stop-band of the Bragg mirror (Fig. 2).

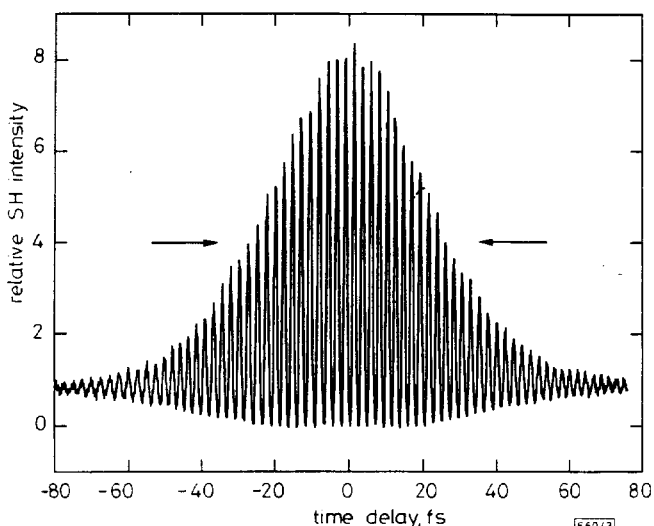


Fig. 3 Interferometric autocorrelation trace of modelocked pulses

Pulse width = 34 fs

The laser cavity is a standard dispersion-compensated delta cavity using fused silica prisms spaced by 40.5 cm. The 2 mm, 0.25%-doped Ti:sapphire crystal is inserted at the Brewster angle between two 10 cm radius high-reflecting (HR) mirrors. We replaced one end mirror by a 30 cm radius HR mirror that focuses the laser mode onto the nonlinear reflector with a 60 μm radius. We obtained a transform-limited pulse width of 34 fs (Fig. 3) with a spectral bandwidth of 22.3 nm (Fig. 2), giving a time-bandwidth product of 0.32, close to an ideal soliton pulse shape. This pulse duration is obtained over practically the full stability regime of the laser cavity, i.e. we could change the distance between the focusing mirror and the saturable absorber over more than 11 mm. Fig. 2 also demonstrates that the pulse duration is limited by the bandwidth of the AlAs/AlGaAs Bragg mirror. It should be possible to

increase the bandwidth of the mirror to support shorter pulse widths, for example by using a chirped mirror design [10]. In addition, the limiting influence of the Bragg mirror can be strongly reduced by an A-FPSA design using the same bottom mirror, but with a thicker GaAs absorber and a high reflecting top mirror. With a 3% output coupler we obtained 140 mW output power with an absorbed pump power of 3 W. The pulse repetition rate was 98.9 MHz which determines the pulse energy density incident on the reflector of 400 μJ/cm² per pulse. This is about 10 times higher than the measured saturation fluence of 350°C GaAs, which means that the saturable absorber is strongly bleached when the laser is modelocked.

We measured the modelocking build-up time using an intracavity chopper and observed the build-up delay between the CW and the second harmonic signal. The build-up time was typically 2.6 μs and insensitive to changes of the cavity stability regime. This is in contrast to much longer build-up times of around 100 μs measured for self-starting KLM, where in addition the alignment tolerances were very critical [4].

The soliton-like pulse is stabilised by the saturable absorber, which we refer to as soliton modelocking [9]. We have shown theoretically that in lasers with strong soliton-like pulse shaping even an absorber with a recovery time significantly longer than the pulsewidth can still stabilise the pulse. Semiconductor absorbers like the one used here typically show a bitemporal pulse response of the absorption recovery: the first, fast decay constant of the order of less than 100 fs is due to intraband thermalisation of the carriers, and the subsequent slow decay constant of 10 ps is due to interband recombination [8]. The slow time constant reliably starts the laser, and the fast recovery time stabilises the soliton-like pulse [9].

Without the nonlinear reflector, we routinely achieved KLM pulses of 17–20 fs length at 800 nm. The KLM is not self-starting and the modelocking process is initiated by a shaking end mirror. In addition, one has to adjust the cavity parameters to tolerances of ~100 μm to achieve strong Kerr lensing and stable short pulses. In contrast with the nonlinear reflector, the modelocking is self-starting without the need of a shaking mirror, and the alignment tolerances are much less critical. Pulses were obtained also in cases where KLM is negligible or even counteracts the pulse formation.

To conclude, we have demonstrated for the first time a self-starting, passively modelocked Ti:sapphire laser using a simple nonlinear semiconductor reflector. Within a build-up time of a few microseconds, we obtained stable 34 fs pulses at an output power of 140 mW over practically the full stability range of the laser cavity.

© IEE 1995

14 December 1994

Electronics Letters Online No: 19950184

L.R. Brovelli, I.D. Jung, D. Kopf, M. Kamp, F.X. Kärtner and U. Keller (Swiss Federal Institute of Technology, Institute of Quantum Electronics, CH-8093 Zurich, Switzerland)

M. Moser (Paul Scherrer institute, CH-8048 Zurich, Switzerland)

References

- 1 SPENCE, D.E., KEAN, P.N., and SIBBETT, W.: '60-fsec pulse generation from a self-mode-locked Ti: sapphire laser', *Opt. Lett.*, 1991, **16**, pp. 42–44
- 2 ZHOU, J., TAFT, G., HUANG, C.-P., MURNANE, M.M., KAPTEYN, H.C., and CHRISTOV, I.P.: 'Pulse evolution in a broad-bandwidth Ti: sapphire laser', *Opt. Lett.*, 1994, **19**, pp. 1149–1151
- 3 LAI, M.: 'Self-starting, self-mode-locked Ti: sapphire laser', *Opt. Lett.*, 1994, **19**, pp. 722–724
- 4 CERULLO, G., SILVESTRI, S.D., and MAGNI, V.: 'Self-starting Kerr lens mode-locking of a Ti: sapphire laser', *Opt. Lett.*, 1994, **19**, pp. 1040–1042
- 5 KELLER, U., CHIU, T.H., and FERGUSON, J.F.: 'Self-starting and self-Q-switching dynamics of a passively modelocked Nd:YLF and Nd:YAG laser', *Opt. Lett.*, 1993, **18**, pp. 217–219
- 6 KELLER, U., MILLER, D.A.B., BOYD, G.D., CHIU, T.H., FERGUSON, J.F., and ASOM, M.T.: 'Solid-state low-loss intracavity saturable absorber for Nd:YLF lasers: an antiresonant semiconductor Fabry-Perot saturable absorber', *Opt. Lett.*, 1992, **17**, pp. 505–507
- 7 KELLER, U.: 'Ultrafast all-solid-state laser technology', *Appl. Phys. B*, 1994, **58**, pp. 347–363
- 8 BROVELLI, L.R., KELLER, U., and CHIU, T.H.: 'Design and operation of antiresonant Fabry-Perot saturable semiconductor absorbers for mode-locked solid-state lasers', *J. Opt. Soc. Am. B*, 1995, **12**

- 9 KÄRTNER, F.X., and KELLER, U.: 'Stabilization of soliton-like pulses with a slow saturable absorber', *Opt. Lett.*, 1995, 20
- 10 FERENCZ, K., and SZIPOCS, R.: 'Recent developments of optical laser coatings in Hungary', *Opt. Eng.*, 1993, 32, pp. 2525-2538

Semiconductor lasers as integrated optoelectronic up/down-converters

E.L. Portnoi, V.B. Gorfinkel, D.A. Barrow, I.G. Thayne, E.A. Avrutin and J.H. Marsh

Indexing terms: Semiconductor junction lasers, Upconversion, Laser modelocking

The use of a semiconductor laser to act as a microwave local oscillator and simultaneously to perform mixing with a high frequency electrical signal is demonstrated experimentally. A particular advantage is that this device produces its output as an optical signal suitable for transmission in fibres.

Introduction: Frequency mixing, along with signal generation and amplification, is one of the basic functions of electronics. All optoelectronic mixers proposed to date produce an electrical intermediate frequency (IF) output [1], whereas the ease with which high-frequencies can be handled optoelectronically suggests that a mixing element is developed which provides its output in the form of an amplitude-modulated optical signal. In this Letter, we demonstrate experimentally the use of a semiconductor laser to perform such an optical mixing operation. Our device is based on the two section semiconductor laser shown schematically in Fig. 1. A saturable absorber in the laser cavity is used to achieve either high frequency modelocking or Q-switching [2], resulting in oscillation of the photon density at frequency f_{LO} . The modal gain of the laser is modulated by applying an electrical signal f_S to the gain section of the laser. Mixing of the optical signal f_{LO} and input signal f_S in the highly nonlinear gain region of the laser results in an optical output signal of frequency f_{OP} at both the sum and difference frequencies ($f_{LO}+f_S$ and $f_{LO}-f_S$).

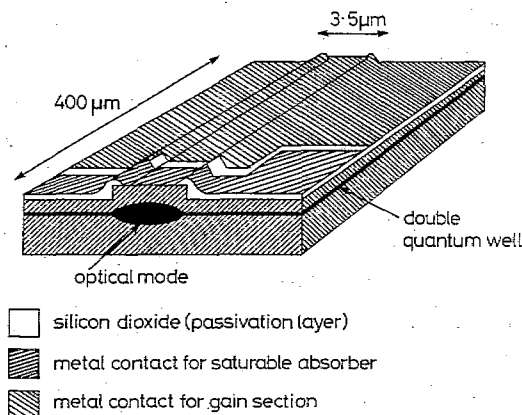


Fig. 1 Schematic diagram of two-section laser used in this study

This mixing scheme is attractive for very high frequencies because it has been shown theoretically that efficient very high-frequency modal gain modulation can be achieved in a four-terminal semiconductor laser structure [3]. Passive modelocking can generate picosecond optical pulses at even higher repetition rates, moving from hundreds of gigahertz [4] to the terahertz range as new techniques [5] are introduced. To show the fundamental principles and for experimental convenience, here we demonstrate mixing at relatively low frequencies of a few gigahertz.

Two section laser: The passively Q-switched laser used in the experiment was based on a ridge waveguide structure with a ridge width of 3.5 μm. The active region consisted of two 6nm thick

strained InGaAs wells separated by 20nm thick GaAs barriers giving an operating wavelength of 960nm. The total cavity length of the device was 400 μm (Fig. 1). The p-type contact was separated into two sections, one forming a contact to the gain section, and the other to an electroabsorption loss modulator (the saturable absorber). The two contacts were electrically isolated by selectively etching a 20 μm gap in the GaAs p⁺ contact layer to give an isolation resistance between the two regions of 2kΩ. The length of the saturable absorber was 30 μm and the threshold current of the device with both sections in forward bias was 9mA.

Measurement system: The self-pulsation frequency of the laser was measured by focusing the CW train of pulses onto a fast InGaAs photodetector with a bandwidth of 20GHz. The electrical signal from the photodiode was then connected to an RF spectrum analyser.

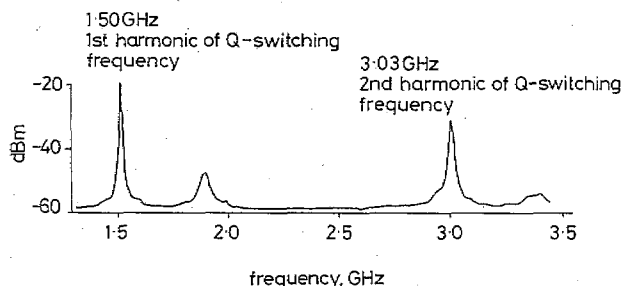


Fig. 2 Frequency spectrum of two-section laser with no RF signal applied to gain section

Results: When driven with a CW current of 80mA through the gain section and 1.6V reverse bias across the saturable absorber, the two-section laser demonstrated Q-switching operation. The Q-switched pulses result in a number of spectral peaks in the frequency domain. The (fundamental) Q-switching frequency of ~1.5 GHz and its second harmonic at 3.0GHz are shown in Fig. 2. Further harmonics were observed at higher frequencies. The smaller peak at 1.88 GHz (25dB below the fundamental Q-switching line f_{LO}) probably arises from reflections in the cables of the measurement system. Note that the amplitude of the second harmonic is ~10dB below that of the fundamental Q-switching line, which shows that the pulses generated are not far from sinusoidal, the measurement system being unlikely to introduce distortions at frequencies measured.

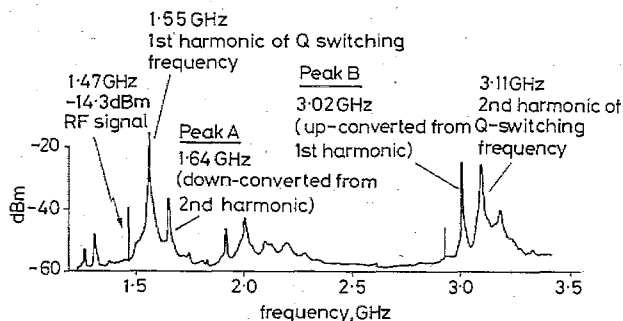


Fig. 3 Frequency spectrum of two-section laser with 1.47GHz RF signal applied to gain section

The addition of an RF signal to the gain section of the laser alters radically the optical output spectrum. Fig. 3 shows the result of applying a -14.3dBm, 1.47GHz RF signal to the gain section. The first point to note is that for -14.3dBm applied RF power, the Q-switching (local oscillator (LO)) frequency is not pulled towards the RF signal frequency, which was the case for higher applied RF powers of more than -5dBm. In the course of these experiments, the Q-switching frequency varied in the range 1.45 - 1.55GHz with no applied RF signal, which we attribute to temperature drift, hence the change in Q-switching frequency between Figs. 2 and 3.